arXiv:1510.04449v1 [cond-mat.quant-gas] 15 Oct 2015

Finite temperature superfluid transition of strongly-correlated lattice bosons in various geometries

T. A. Zaleski*, T. K. Kopeć
Institute for Low Temperature and Structure Research Polish Academy of Sciences, POB 1410, 50-950 Wrocław 2, Poland

We study finite-temperature properties of the strongly interacting bosons in three-dimensional lattices by employing the combined Bogoliubov method and the quantum rotor approach. Based on the mapping of the Bose-Hubbard Hamiltonian of strongly interacting bosons onto U(1) phase action, we study their thermodynamic phase diagrams for several lattice geometries including; simple cubic, body- as well as face-centered lattices. The quantitative values for the phase boundaries obtained here may be used as a reference for emulation of the Bose-Hubbard model on a variety of optical lattice structures in order to demonstrate experimental-theoretical consistency for the numerical values regarding the location of the critical points.

I. INTRODUCTION

It is well known that the ground state of a system of repulsively interacting bosons in a periodic potential can be either in a superfluid state or in a Mott-insulting state, characterized by integer boson densities and the existence of a gap for particle-hole excitations [1]. One key piece of evidence for the Mott insulator phase transition is the loss of global phase coherence of the matter wave function. However, there are many possible sources of phase decoherence in these systems. Substantial decoherence can be induced by quantum or thermal depletion of the condensate. Experimentally, an enormous progress was made in the experimental study of cold atoms in optical lattices [2]. Cold atoms interacting with a spatially modulated optical potential resemble in many respects electrons in ion-lattice potential of a solid crystals. However, optical lattices have several advantages with respect to solid state systems. They can be made to be largely free from defects and can be controlled very easily by changing the laser field properties. Finally, ultra-cold atoms confined in optical lattice structure provide a very clean experimental realization of a strongly correlated many-body problem [3]. Moreover, in contrast to solids, where the lattice spacings are generally of order of Angstrom units, the lattice constants in optical lattices are typically three order of magnitude larger. Furthermore, variety of multi-dimensional lattices can be experimentally obtained by appropriate setup of laser beams including cubic face-centered and body-centered lattices [4, 5]. For example, a three dimensional (3D) lattice can be created by the interference of at least six orthogonal sets of counter propagating laser beams. Although the initial system can be prepared at a relatively low temperature, the ensuing system after ramp-up of the lattice has a temperature which is usually higher due to adiabatic and other heating mechanisms. Recent experiments have reported temperatures on the order of $k_BT \sim 0.9t$ where t, the hopping parameter, measures the kinetic energy of bosons [6]. At such temperatures, the effects of excited states become important, motivating investigations of the the *finite* temperature phase diagrams, showing the interplay between quantum and thermal fluctuations.

Therefore, the goal of this paper is to provide a study of the combined effects of a confining lattice potential and finite temperature on the state diagram of the Bose-Hubbard model in three dimensions in strongly correlated regime where the standard Bogoliubov treatment fails to describe the system and a more general framework is required. Usually, studies of bosons in optical lattices have been conducted at zero temperature and in two dimensional systems, dealing with Mott insulator-superfluid transition. In the present work, we explore the phase transition from the Mott to the superfluid state in a system of strongly interacting bosons on a cubic lattice with the chemical potential and temperature as the control parameters. Furthermore, we employ the quantum rotor method, which uses the module–phase representation of strongly correlated bosons. This introduces a conjugate to the density of bosons U(1) quantum phase variable, which acquires dynamic significance from the boson-boson interaction. The quantum rotor approach has been verified with other methods [7], like quantum Monte Carlo [8] or DMFT [9] giving coinciding results.

The plan of the paper is as follows: in Section II, we introduce the microscopic Bose-Hubbard model relevant for the description of strongly interacting bosons. Furthermore, in the following Section, we briefly present technical aspects our quantum rotor approach and in Section IV we calculate the temperature phase diagrams. Finally, we conclude in the Section V.

II. MODEL HAMILTONIAN

The simplest non trivial model that describes interacting bosons in a periodic potential is the Bose Hubbard Hamiltonian. It includes the main physics that describe strongly interacting bosons, which is the competition be-

*Corresponding author. Tel.: +48 713435021; fax: +48 713441029.
E-mail address: t.zaleski@int.pan.wroc.pl (T.Zaleski).

tween kinetic and interaction energy. The realization of the Bose-Hubbard Hamiltonian using optical lattices has the advantage that the interaction matrix element U and the tunneling matrix element t can be controlled by adjusting the intensity of the laser beams. Its Hamiltonian in a second quantized form reads:[1]

$$\begin{aligned}\mathcal{H} &= -t\sum_{\langle \mathbf{r},\mathbf{r}'\rangle}\left[a^{\dagger}(\mathbf{r})\,a(\mathbf{r}')+a^{\dagger}(\mathbf{r}')\,a(\mathbf{r})\right]\\ &+\frac{U}{2}\sum_{\mathbf{r}}n^{2}(\mathbf{r})-\overline{\mu}\sum_{\mathbf{r}}n(\mathbf{r}).\end{aligned}\tag{1}$$

The first term is the kinetic energy of bosons moving in a given lattice within a tight-binding scheme, where t represents nearest neighbors tunneling matrix, $\mathbf{r}$ and $\mathbf{r}'$ are lattice sites and $\langle \mathbf{r},\mathbf{r}'\rangle$ denotes summation over nearest neighbors. The following introduces inter-bosonic correlations with U being the strength of the on-site repulsive interaction of bosons. Furthermore, $\overline{\mu}=\mu+\frac{U}{2}$, where μ is a chemical potential controlling the average number of bosons. The operators $a^{\dagger}(\mathbf{r})$ and $a(\mathbf{r}')$ create and annihilate bosons, while the boson number operator $n(\mathbf{r})=a^{\dagger}(\mathbf{r})\,a(\mathbf{r})$ and a total number of sites is equal to N. The Hamiltonian and its descendants have been widely studied within the last years. The phase diagram and ground-state properties include the mean-field ansatz,[1] strong coupling expansions,[10–12] the quantum rotor approach,[13] methods using the density matrix renormalization group DMRG,[14–17] and quantum Monte Carlo QMC simulations.[18**?** –20]

III. U(1) QUANTUM ROTOR FORMULATION

The quartic form of the Hamiltonian makes it very difficult to deal with it in all the different regimes. The aim of this chapter is to rewrite it so that a systematic approach can be developed to accommodate strongly interacting regime, In the following, we use a theory that goes beyond the simple Bogoliubov approximation which has been recently developed that incorporates the phase degrees of freedom via the quantum rotor approach to describe regimes beyond the very weakly interacting one [21]. This scenario provided a picture of quasi-particles and energy excitations in the strong interaction limit, where the transition between the superfluid and the Mott state is be driven by phase fluctuations. Taking advantage of the macroscopically populated condensate state, we have separated the problem into the amplitude of the Bose field and the fluctuating phase that was absent in the original Bogoliubov problem [22].

The statistical sum of the system defined by Eq. (1) can be written in a path integral form with use of complex fields, $a(\mathbf{r}\tau)$ depending on the "imaginary time" $0\leq\tau\leq\beta\equiv 1/k_{B}T$, (with T being the temperature) that satisfy the periodic condition $a(\mathbf{r}\tau)=a(\mathbf{r}\tau+\beta)$:

$$Z=\int\left[\mathcal{D}\overline{a}\mathcal{D}a\right]e^{-\mathcal{S}[\overline{a},a]},\tag{2}$$

where the action $\mathcal{S}$ is equal to:

$$\mathcal{S}\left[\overline{a},a\right]=\int_{0}^{\beta}d\tau\mathcal{H}(\tau)+\mathcal{S}_{\mathcal{B}}\left[\overline{a},a\right],\tag{3}$$

where the Berry term is:

$$\mathcal{S}_{\mathcal{B}}\left[\overline{a},a\right]=\sum_{\mathbf{r}}\int_{0}^{\beta}d\tau\overline{a}(\mathbf{r}\tau)\frac{\partial}{\partial\tau}a(\mathbf{r}\tau).$$

Now, we are briefly introducing the quantum rotor approach.[23] The fourth-order term in the Hamiltonian in Eq. (1) can be decoupled using the Hubbard-Stratonovich transformation with an auxiliary field $V(\mathbf{r}\tau)$:

$$\begin{aligned}&e^{-\frac{U}{2}\sum_{\mathbf{r}}\int_{0}^{\beta}d\tau n^{2}(\mathbf{r}\tau)}\\ &\propto\int\frac{\mathcal{D}V}{\sqrt{2\pi}}e^{\sum_{\mathbf{r}}\int_{0}^{\beta}d\tau\left[-\frac{V^{2}(\mathbf{r}\tau)}{2U}+iV(\mathbf{r}\tau)n(\mathbf{r}\tau)\right]}.\end{aligned}\tag{4}$$

The fluctuating "imaginary chemical potential" $iV(\mathbf{r}\tau)$ can be written as a sum of static $V_{0}(\mathbf{r})$ and periodic function:

$$V(\mathbf{r}\tau)=V_{0}(\mathbf{r})+\delta V(\mathbf{r}\tau),\tag{5}$$

where, using Fourier series:

$$\delta V(\mathbf{r}\tau)=\frac{1}{\beta}\sum_{\ell=1}^{\infty}\delta V(\mathbf{r}\omega_{\ell})\left(e^{i\omega_{\ell}\tau}+e^{-i\omega_{\ell}\tau}\right),\tag{6}$$

with the Bose-Matsubara frequencies are $\omega_{\ell}=2\pi\ell/\beta$ and $\ell=0,\pm1,\pm2,\ldots$.

A. Phase action

Introducing the U(1) phase field $\phi(\mathbf{r}\tau)$ via the Josephson-type relation:

$$\dot{\phi}(\mathbf{r}\tau)=\delta V(\mathbf{r}\tau)\tag{7}$$

with $\dot{\phi}(\mathbf{r}\tau)=\partial\phi(\mathbf{r}\tau)/\partial\tau$ we can now perform a local gauge transformation to new bosonic variables:

$$a(\mathbf{r}\tau)=b(\mathbf{r}\tau)\,e^{i\phi(\mathbf{r}\tau)},\tag{8}$$

where:

$$\zeta(\mathbf{r}\tau)=e^{i\phi(\mathbf{r}\tau)}\tag{9}$$

with $\phi(\mathbf{r}\tau)$ being U(1) phase variable. Concerning the amplitude in Eq. (8), the operator splits into a sum:

$$b(\mathbf{r}\tau)=b_{0}+\delta b(\mathbf{r}\tau).\tag{10}$$

Since, the strongly correlated limit is dominated by phase fluctuations, we neglect a contribution coming

from $\delta b\left(\mathbf{r}\tau\right)$ in subsequent calculations. After the variable transformations the statistical sum becomes:

$$Z=\int\left[\mathcal{D}\bar{b}\mathcal{D}b\right]\left[\mathcal{D}\phi\right]e^{-\mathcal{S}\left[\bar{b},b,\phi\right]} \tag{11}$$

with the action:

$$\begin{aligned}\mathcal{S}\left[\overline{b},b,\phi\right]&=\mathcal{S}_{0}\left[\phi\right]+\mathcal{S}_{\mathcal{B}}\left[\overline{b},b\right]\\&-t\sum_{\left\langle\mathbf{r},\mathbf{r}'\right\rangle}\int_{0}^{\beta}d\tau\left[e^{i\phi\left(\mathbf{r}'\tau\right)-i\phi\left(\mathbf{r}\tau\right)}\overline{b}\left(\mathbf{r}\tau\right)b\left(\mathbf{r}'\tau\right)+h.c.\right]\\&+\sum_{\mathbf{r}}\int_{0}^{\beta}d\tau\left[U\left|b_{0}\right|^{2}-\overline{\mu}\right]\overline{b}\left(\mathbf{r}\tau\right)b\left(\mathbf{r}\tau\right)\end{aligned} \tag{12}$$

and

$$\mathcal{S}_{0}\left[\phi\right]=\sum_{\mathbf{r}}\int_{0}^{\beta}d\tau\left[\frac{\dot{\phi}^{2}\left(\mathbf{r}\tau\right)}{2U}+i\frac{\overline{\mu}}{U}\dot{\phi}\left(\mathbf{r}\tau\right)\right]. \tag{13}$$

The statistical sum can be integrated over the phase or bosonic variables with the phase or bosonic action:

$$\mathcal{S}\left[\phi\right]=-\ln\int\left[\mathcal{D}\bar{b}\mathcal{D}b\right]e^{-\mathcal{S}\left[\bar{b},b,\phi\right]}, \tag{14}$$

so that:

$$Z=\int\left[\mathcal{D}\phi\right]e^{-\mathcal{S}\left[\phi\right]}. \tag{15}$$

In performing the integration in Eq. (15) one should take phase configurations that satisfy the boundary condition $\phi\left(\mathbf{r}\beta\right)-\phi\left(\mathbf{r}0\right)=2\pi m\left(\mathbf{r}\right)$ and $m\left(\mathbf{r}\right)=0,\pm1,\pm2,\ldots$. The phase-only action from Eq. (13) can be written explicitly:

$$\mathcal{S}\left[\phi\right]=\mathcal{S}_{0}\left[\phi\right]+J\sum_{\left\langle\mathbf{r},\mathbf{r}'\right\rangle}\int_{0}^{\beta}d\tau\cos\left[\phi\left(\mathbf{r}\tau\right)-\phi\left(\mathbf{r}'\tau\right)\right], \tag{16}$$

where $J=t\left|b_{0}\right|^{2}$ represents the stiffness for the phase field.

B. Phase coherence and order parameter

The superfluid order parameter is defined by:

$$\Psi_{B}=\left\langle a\left(\mathbf{r}\tau\right)\right\rangle=\left\langle b\left(\mathbf{r}\tau\right)\right\rangle\psi_{B}\equiv\left|b_{0}\right|^{2}\psi_{B}, \tag{17}$$

where $\langle\ldots\rangle$ denotes the averaging over effective action depending on pertinent variables. However, a nonzero value of the amplitude $\left\langle b\left(\mathbf{r}\tau\right)\right\rangle$ is not sufficient for superfluidity. Also, the U(1) phase variables must become coherent, which leads to the phase order parameter:

$$\psi_{B}=\left\langle e^{i\phi\left(\mathbf{r}\tau\right)}\right\rangle. \tag{18}$$

which is equal to zero in the disordered phase (in particular, the Mott-insulator for $T=0$). We introduce a unimodular scalar field $\zeta\left(\mathbf{r}\tau\right)=e^{i\phi\left(\mathbf{r}\tau\right)}$ using the identity:

$$\begin{aligned}1\equiv\int\left[\mathcal{D}^{2}\zeta\right]\prod_{\mathbf{r}}\delta\left[\zeta\left(\mathbf{r}\tau\right)-e^{i\phi\left(\mathbf{r}\tau\right)}\right]\\\delta\left[\overline{\zeta}\left(\mathbf{r}\tau\right)-e^{-i\phi\left(\mathbf{r}\tau\right)}\right].\end{aligned} \tag{19}$$

This leads us to the partition function:

$$Z=\int\left[\mathcal{D}^{2}\zeta\right]\delta\left[\sum_{\mathbf{r}}\left|\zeta\left(\mathbf{r}\tau\right)\right|^{2}-N\right]e^{-\mathcal{S}\left[\zeta,\overline{\zeta}\right]}, \tag{20}$$

where the unimodularity condition was weakened to be fulfilled on average and is imposed by a Lagrange multiplier λ with the Laplace transform $\delta\left(x\right)=\int d\lambda e^{\lambda x}$. The action:

$$\mathcal{S}\left[\zeta,\overline{\zeta}\right]=\frac{1}{\beta N}\sum_{\mathbf{k}\ell}\overline{\zeta}_{\mathbf{k}}\left(\omega_{\ell}\right)\Gamma_{\lambda_{0}}^{-1}\left(\mathbf{k}\omega_{\ell}\right)\zeta_{\mathbf{k}}\left(\omega_{\ell}\right), \tag{21}$$

with the propagator:

$$\Gamma_{\lambda_{0}}^{-1}\left(\mathbf{k}\omega_{l}\right)=\lambda_{0}-J\left(\mathbf{k}\right)+K^{-1}\left(\omega_{\ell}\right). \tag{22}$$

The Fourier transform of the inverse of the phase-phase correlator $K\left(\tau-\tau'\right)=\left\langle e^{i\phi\left(\mathbf{r}\tau\right)-i\phi\left(\mathbf{r}\tau'\right)}\right\rangle$ depending on a single site only with the average respective to the phase action only (see, Ref. [21]) reads:

$$K^{-1}\left(\omega_{\ell}\right)=\frac{U}{4}-U\left[v\left(\frac{\overline{\mu}}{U}\right)+\frac{i\omega_{\ell}}{U}\right]^{2}, \tag{23}$$

while $J\left(\mathbf{k}\right)=2tb_{0}^{2}\varepsilon_{\mathbf{k}}$, $\varepsilon_{\mathbf{k}}$ is the dispersion of a given lattice, b_{0} is the bosonic amplitude obtained from minimalizaition of the Hamiltonian $\partial\mathcal{H}\left(b_{0}\right)/\partial b_{0}=0$:

$$b_{0}^{2}=\frac{zt}{U}+\frac{\overline{\mu}}{U}, \tag{24}$$

z is a lattice coordination number and, finally, $v(x)=x-[x]-1/2$, with $[x]$ being the floor function, which gives the greatest integer less than or equal to x resulting from the periodicity of the phase variable. In the large-N limit, the value of the Lagrange multiplier λ can be determined from the saddle point method

$$\left.\frac{\partial\mathcal{S}}{\partial\lambda}\right|_{\lambda=\lambda_{0}}=0 \tag{25}$$

with the stationary point value λ_{0}. Explicitly, from Eq. (25) it follows that:

$$1=\left\langle\overline{\zeta}\left(\mathbf{r}\tau\right)\zeta\left(\mathbf{r}\tau\right)\right\rangle=\frac{1}{\beta N}\sum_{\mathbf{k}\ell}\Gamma_{\lambda_{0}}\left(\mathbf{k}\omega_{\ell}\right). \tag{26}$$

However, in the presence of the condensate, in the ordered phase, the average unimodularity condition in Eq.

(26) is depleted by the presence of the order parameter so that:

$$1-\psi_B^2=\frac{1}{\beta N}\sum_{\mathbf{k}\ell}\Gamma_{\lambda_{0c}}\left(\mathbf{k}\omega_\ell\right), \tag{27}$$

where the saddle point value λ_{0c} at the critical point and in the ordered phase, is fixed by the condition:

$$\Gamma^{-1}_{\lambda_{0c}}\left(\mathbf{k}=0,\omega_\ell=0\right)=0, \tag{28}$$

which physically means the divergence of the inverse of the uniform static order parameter susceptibility.

Explicitly, summing over Matsubara frequencies, the Eq. (26) becomes:

$$1-\psi_B^2=\frac{U}{4N}\sum_{\mathbf{k}}\frac{\coth\left(\frac{1}{2}\beta\Xi_{\mathbf{k}}^-\right)+\coth\left(\frac{1}{2}\beta\Xi_{\mathbf{k}}^+\right)}{\Xi_{\mathbf{k}}}, \tag{29}$$

where:

$$\Xi_{\mathbf{k}}=U\sqrt{\frac{\lambda_0-\lambda_{0c}}{U}+\frac{2t}{U}b_0^2\left(\varepsilon_{\mathbf{0}}-\varepsilon_{\mathbf{k}}\right)+v^2\left(\frac{\overline{\mu}}{U}\right)},$$
$$\Xi_{\mathbf{k}}^{\pm}=\Xi_{\mathbf{k}}\pm Uv\left(\frac{\overline{\mu}}{U}\right). \tag{30}$$

In the next Section we explicitly calculate the outcome of the equation (29) for several three dimensional lattice geometries.

IV. RESULTS

In this Section, we first specify the corresponding lattice structure factors defined as

$$\varepsilon_{\mathbf{k}}^{\mathrm{X}}=\sum_{\{\mathbf{d}\}_{\mathrm{X}}}\cos\left(d_xk_x+d_yk_y+d_zk_z\right), \tag{31}$$

where $\{\mathbf{d}\}_{\mathrm{X}}$ denotes a set of vectors connecting a given site of a lattice X and its nearest neighbors. It should be noted that in this sense the geometry of the lattice results from locations of bonds between nearest neighbors for a chosen lattice site (given by $\{\mathbf{d}\}_X$) rather than just simply the location of the lattice sites.

Geometries that we use, are presented in Fig. 1. Simple cubic lattice (SC) with the coordination number $z=6$ is defined by the set of vectors

$$\{\mathbf{d}\}_{\mathrm{SC}}=\{(\pm1,0,0),(0,\pm1,0),(0,0,\pm1)\} \tag{32}$$

giving

$$\varepsilon_{\mathbf{k}}^{\mathrm{SC}}=\cos k_x+\cos k_y+\cos k_z. \tag{33}$$

For face centered lattice (FCC) with the coordination $z=12$ one has

$$\{\mathbf{d}\}_{\mathrm{FCC}}=\{(\pm1,\pm1,0),(\pm1,0,\pm1),(0,\pm1,\pm1)\} \tag{34}$$

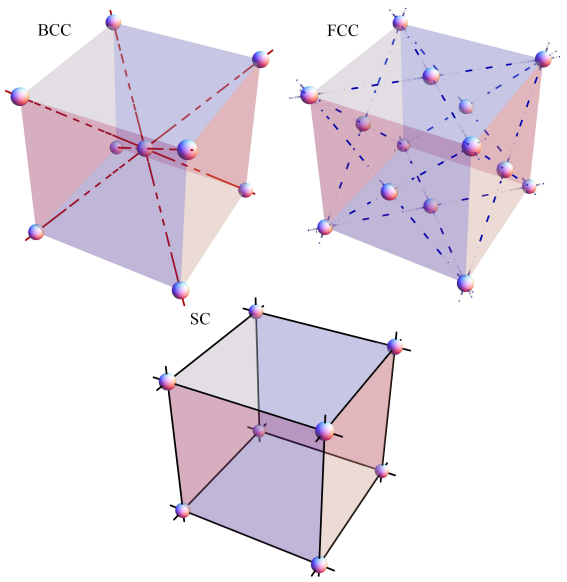

Figure 1: (Color online) Various geometries of three-dimensional lattices: SC (simple cubic), BCC (body-centered cubic) and FCC (face-centered cubic). Bonds between the nearest neighbors are denoted by lines (solid or dashed) and are located along: the lattice axes (SC), diagonals of the lattice planes (FCC) and the main diagonals (BCC), respectively.

and correspondingly

$$\varepsilon_{\mathbf{k}}^{\mathrm{FCC}}=2\left(\cos k_x\cos k_z+\cos k_x\cos k_y+\cos k_y\cos k_z\right) \tag{35}$$

Furthermore, we consider body centered lattice (BCC), where $z=8$ and $\{\mathbf{d}\}_{\mathrm{BCC}}$ is given by

$$\{\mathbf{d}\}_{\mathrm{BCC}}=\{(\pm1,\pm1,\pm1)\} \tag{36}$$

so that

$$\varepsilon_{\mathbf{k}}^{\mathrm{BCC}}=4\cos k_x\cos k_y\cos k_z. \tag{37}$$

As temperature increases, thermal fluctuations melt away both the SF and MI phases, introducing the normal (N) phase. For higher temperatures, the critical coupling $(U/t)_c$ for the SF-N transition is lowered (see, Fig. 2). With increasing temperature, the superfluid regions in between the Mott lobes shrink in width and shift to larger tunneling energies (see, Fig. 2 for the FCC lattice phase diagram). The phase diagram includes two different types of phase transition. One type takes place at any generic point of the phase boundary, and it is driven by the energy cost to add or subtract small numbers of particles to the incompressible Mott state as explained above. On the other hand, the other type only occurs at fixed integer density and takes place at the tip of the lobes. This transition is driven at fixed density by decreasing U/t and enabling the bosons to overcome the on site repulsion. The two kinds of phase transition belong

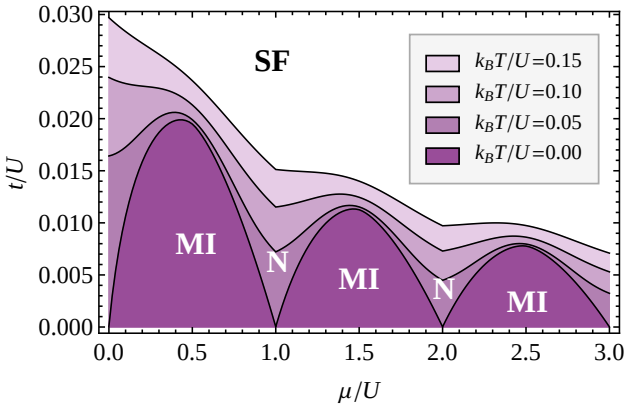

Figure 2: (Color online) Coupling ratio t/U vs. chemical potential μ/U phase diagram in various temperatures for the face-centered cubic lattice (FCC).

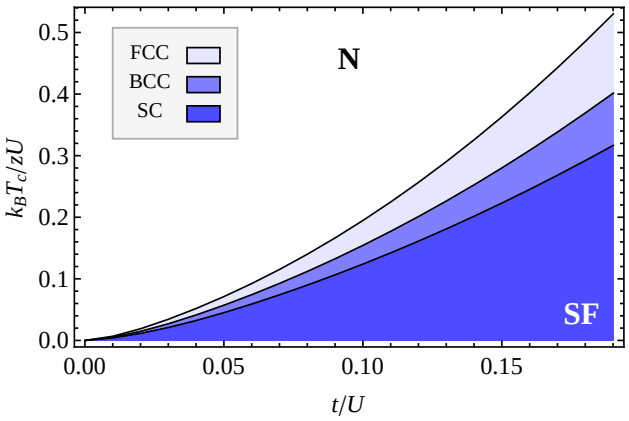

Figure 3: (Color online) Critical temperature k_BT/U as a function of the coupling ratio t/U for $\mu/U = 1$ and various lattice geometries (as denoted in the text).

to different universality classes. In the $T \to 0$ limit, the propagator in Eq. (22) becomes:

$$\Gamma_{\mathbf{k}}^{-1}(\omega_\ell) = r + \mathbf{k}^2 + \omega_\ell^2 + i\omega_\ell + v\left(\frac{\overline{\mu}}{U}\right). \qquad (38)$$

Here, $r \sim 2tb_0^2\varepsilon_{\mathbf{0}} - \lambda$ is the critical "mass" parameter that vanishes at the phase transition boundary and $\mathbf{k}^2 = k \cdot k$. Due to the quantum nature of the problem, the scaling of the spatial degrees of freedom $\mathbf{k} \to \mathbf{k}' = s\mathbf{k}$ implies the scaling for frequencies in a form $\omega_\ell \to \omega'_\ell = s^z\omega_\ell$ with the dynamical critical exponent z. At the tips of the lobes in the t/U-μ/U phase diagram (see, Fig. 2), one has $v(\overline{\mu}/U) = 0$, so that $\Gamma_{\mathbf{k}}^{-1}(\omega_\ell) \sim k^2 + \omega_\ell^2$, with space-time isotropy giving $z = 1$. However, the other points on the critical line with nonvanishing $v(\mu/U)$ reflect the absence of the particle-hole symmetry due to the imaginary term involving $i\omega_\ell$. In this case, the higher order term involving ω_ℓ^2 becomes irrelevant and can be ignored, while the critical form of the propagator in Eq. (38) reads $\Gamma_{\mathbf{k}}^{-1}(\omega_\ell) \sim k^2 + iv(\overline{\mu}/U)\omega_\ell$. Now, the scaling requires $z = 2$ as a result of the momentum-frequency anisotropy.

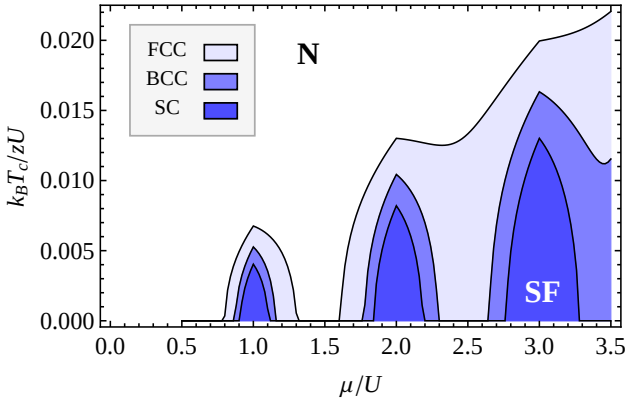

Figure 4: (Color online) Dependence of critical temperature k_BT/U on the chemical potentialμ/U for $t/U = 0.01$ and various lattice geometries (as denoted in the text).

The superfluid critical temperature T_c is strongly dependent on the geometry of the lattice: T_c is the highest for the FCC and is decreasing for BCC and SC lattice, respectively. It can be also observed in temperature-chemical doping diagrams (see, Fig. 4): the FCC lattice requires much higher temperature to destroy the superfluid phase than the BCC and SC . The ability of the FCC lattice to offer the highest critical temperature is quite expected. The lattice has $z = 12$ nearest neighbors, as compared to 8 and 6 for BCC and SC lattices, respectively. We note, that in the mean-field theory, the critical temperature is simply proportional to the number of the nearest neighbors [27]. Here, however, the critical temperature is already normalized by the z factor (see, Figs. 3 and 4). Therefore our findings, which are based on a more accurate approach, show that the lattice topology has an additional influence on equilibrium properties of the Bose-Hubbard model, which are worth to be tested experimentally.

V. CONCLUSIONS

In this paper, we have determined the combined effects of three dimensional lattice potential trapping and temperature for a system of strongly interacting bosons on several lattice structures. Usually, to be able to talk about temperature, it is necessary to have a closed system in thermal equilibrium with a thermal bath. In optical lattices, the role of the thermal bath is played by the photons. Although, they do not give the thermal contact and heat exchange required, the reduction of the entropy of the system is achieved at the expense of the entropy of the photons. Therefore, the use of the term "temperature" is fully justified. As our calculation exemplify, the finite temperature equilibrium state is marked by the competing effects of thermally driven phase fluctuations and phase locking due to hopping of bosons.

Thus, the precise manipulation of this form of matter is of considerable experimental and theoretical interest. Finally, regarding the theoretical aspect of our work, it would be also desirable to test of the method presented by comparing it against numerical solutions obtained by e.g. diagonalizing the Bose-Hubbard Hamiltonian for a moderate number of atoms and wells.

Acknowledgments

We would like to acknowledge support from the Polish National Science Centre (Grant No. 2011/03/B/ST3/00481).

VI. APPENDIX

Introducing the density of states:

$$\rho_{\mathrm{X}}(x)=\frac{1}{N}\sum_{\mathbf{k}}\delta\left(x-\varepsilon_{\mathbf{k}}^{\mathrm{X}}\right) \tag{39}$$

can greatly simplify numerical calculations, as it converts multiple sums over wave vectors into a linear integral over a bandwidth [e.g., in Eq. (29)]. Here, the index X stands for SC, FCC or BCC lattices and in several cases a close-form formula for $\rho_{\mathrm{X}}(x)$ can be found. Using the dispersion relation from Section IV we enumerate in the following the relevant cases.

For the simple cubic lattice one has:

$$\rho_{\mathrm{SC}}(x)=\frac{1}{\pi^3}\int_{\max(-1,-2-x)}^{\min(1,2-x)}\frac{du}{\sqrt{1-u^2}}\times\mathbf{K}\left[\sqrt{1-\left(\frac{x+u}{2}\right)^2}\right]\Theta\left(3-|x|\right). \tag{40}$$

where $\mathbf{K}(x)$ stands for the elliptic integral of the first kind [28] and $\Theta(x)$ is the unit step function. The density of states for the body centered lattice is given by

$$\rho_{\mathrm{BCC}}(4x)=\frac{1}{2\pi^3}\left\{\mathbf{K}^2\left[\sqrt{\frac{1}{2}\left(1+\sqrt{1-x^2}\right)}\right]-\mathbf{K}^2\left[\sqrt{\frac{1}{2}\left(1-\sqrt{1-x^2}\right)}\right]\right\}\Theta\left(1-|x|\right). \tag{41}$$

The formula for the face centered lattice is a bit more involved,

$$\rho_{\mathrm{FCC}}(2x)=\frac{1}{2\pi}\lim_{\delta\to 0}\mathrm{Im}G(x-i\delta) \tag{42}$$

where $G(x)$ is given by:

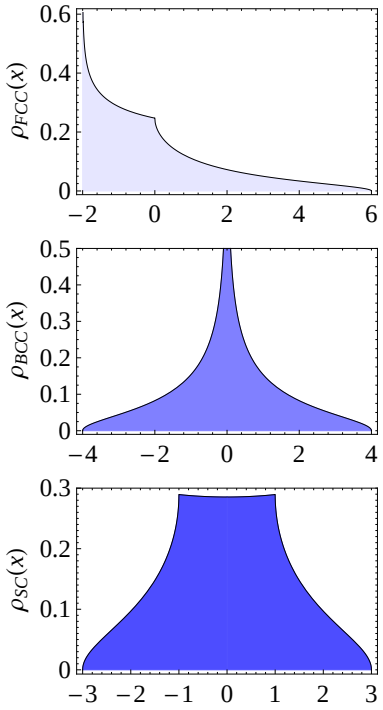

Figure 5: (Color online) Densities of states of the three-dimensional lattices: simple cubic (SC), face-centered cubic (FCC) and body-centered cubic (BCC).

for $-1\leq x<0$):

$$G(x)=\frac{8}{\pi^3(x+1)}\int_{\arccos\left(\frac{1-x}{2}\right)}^{\arccos\left(\sqrt{-x}\right)}du\mathbf{K}\left[1-k^2(x,u)\right]+\frac{4}{\pi^3(x+1)}\int_0^{\arccos\left(\frac{1-x}{2}\right)}\frac{du}{k(x,u)}\mathbf{K}\left[\frac{\sqrt{k^2(x,u)-1}}{k(x,u)}\right]+\frac{8}{\pi^3(x+1)}\int_{\arccos\left(\sqrt{-x}\right)}^{\pi/2}du\mathbf{K}\left[\frac{1}{1-k^2(x,u)}\right], \tag{43}$$

for $0\leq x<1$:

$$G(x)=\frac{8}{\pi^3(x+1)}\int_{\arccos\left(\frac{1-x}{2}\right)}^{\pi/2}du\mathbf{K}\left[1-k^2(x,u)\right]+\frac{4}{\pi^3(x+1)}\int_0^{\arccos\left(\frac{1-x}{2}\right)}du\mathbf{K}\left[\frac{1}{1-k^2(x,u)}\right], \tag{44}$$

and for $1\leq x<3$:

$$G(x)=\frac{4}{\pi^3(x+1)}\int_0^{\arccos\left(\frac{1-x}{2}\right)}du\frac{\mathbf{K}\left[\frac{\sqrt{k^2(x,u)-1}}{k(x,u)}\right]}{k(x,u)}, \tag{45}$$

where

$$k(x,u)=\frac{2\sqrt{x+\cos^2(u)}}{u+1}. \tag{46}$$

In Fig. 5 we have plotted the outcome for $\rho_{\rm X}(x)$ regarding the employed lattices.

[1] M. P. A. Fisher, P. B. Weichman, G. Grinstein, and D. S. Fisher, Phys. Rev. B **40**, 546 (1989).
[2] M. Greiner, O. Mandel, T. Esslinger , T. W. Hänsch, and I. Bloch, Nature **415**, 39 (2002).
[3] I. Bloch, Nat. Phys. **1**, 23 (2005).
[4] K. I. Petsas, A. B. Coates, and G. Grynberg, Phys. Rev. A **50**, 5173 (1994).
[5] W. Kim, C. Park, J.-R. Kim, Y. Choi, S. Kang, S. Lim, Y.-L. Lee, J. Ihm, and K. An, Nano Lett. **11**, 729 (2011).
[6] K. Jimenez-Garcia, R. L. Compton, Y.-J. Lin, W. D. Phillips, J. V. Porto, and I. B. Spielman, Phys. Rev. Lett. **105**, 110401 (2010).
[7] T. P. Polak and T. K. Kopeć, J. Phys. B. **42**, 095302 (2009); T. A. Zaleski and T. P. Polak, Phys. Rev. A **83**, 023607 (2011).
[8] B. Capogrosso-Sansone, N. V. Prokof'ev, and B. V. Svistunov, Phys. Rev. B **75**, 134302 (2007).
[9] P. Anders, E. Gull, L. Pollet, M. Troyer and P. Werner, New J. Phys. **13**, 075013 (2011).
[10] J. K. Freericks and H. Monien, Phys. Rev. B **53**, 2691 (1996).
[11] N. Elstner and H. Monien, Phys. Rev. B **59**, 12184 (1999).
[12] J. K. Freericks, H. R. Krishnamurthy, Y. Kato, N. Kawashima, and N. Trivedi, Phys. Rev. A **79**, 053631 (2009).
[13] T. A. Zaleski and T. K. Kopeć, J. Phys. A: Math. Theor. **43**, 425303 (2010).
[14] T. D. Kühner and H. Monien, Phys. Rev. B **58**, R14741 (1998).
[15] S. Rapsch, U. Schollwöck, and W. Zwerger, Europhys. Lett. **46**, 559 (1999).
[16] C. Kollath, U. Schollwöck, J. von Delft, and W. Zwerger, Phys. Rev. A **69**, 031601(R) (2004).
[17] C. Kollath, A. M. Läuchli, and E. Altman, Phys. Rev. Lett. **98**, 180601 (2007).
[18] G. G. Batrouni and R. T. Scalettar, Phys. Rev. B **46**, 9051 (1992).
[19] S. Wessel, F. Alet, M. Troyer, and G. G. Batrouni, Phys. Rev. A **70**, 053615 (2004).
[20] B. Capogrosso-Sansone, S. G. Söyler, N. Prokof'ev, and B. Svistunov, Phys. Rev. A **77**, 015602 (2008).
[21] T. A. Zaleski, and T. K. Kopeć, Phys. Rev. A **84**, 053613 (2011).
[22] N. N. Bogoliubov, J. Phys. Moscow 11, 23 (1947).
[23] T. P. Polak and T. K. Kopeć, Phys. Rev. B **76**, 094503 (2007).
[24] C. G. Callan, R. F. Dashen, and D. J. Gross, Phys. Lett. **63B**, 334 (1976).
[25] M. V. Berry, Proc. R. Soc. London, Ser. A **392**, 451 (1984).
[26] G. Veneziano, Nucl. Phys. B **159**, 213 (1979).
[27] F. Gerbier, Phys. Rev. Lett. **99**, 120405 (2007).
[28] M. Abramovitz and I. Stegun, *Handbook of Mathematical Functions* (Dover, New York, 1970).